Chapter 11
Surfaces

Gott schuf das Volumen, der Teufel die Oberfläche.
God created the bulk; surfaces were made by the devil.

attributed to W. Pauli

Abstract The specifics of semiconductors surfaces, their symmetry, equilibrium crystal shape, reconstructions, steps and faceting are summarized, being important for epitaxy. Physical surface properties such as vibrational and electronic states are discussed.

11.1 Introduction

Obviously every crystal has a surface all around it, connecting it to the surrounding world. This represents a brutal perturbation of the bulk periodicity with the consequence of a whole new world of physics at the surface. With regard to semiconductor technology, the surface properties are of large importance in a number of instances:

- The crystal growth of semiconductors always occurs at a surface. This subject will be discussed in Chap. 12.
- The surface is subject to interaction with the chemistry of the surrounding atmosphere. This is of essential importance for catalysis, e.g., oxidation of CO at noble metals or photocatalytic water splitting, e.g., using TiO_2, into oxygen and hydrogen [1051, 1052]. Photocatalysis is briefly discussed in Sect. 22.1. The interaction and reaction with the surrounding atmosphere can lead modifications of the semiconductor such as change of conductivity, e.g.., in SnO_2, which can be used in the construction of gas detectors [1053–1055].
- Surface passivation and barriers, e.g., using photoresist, silicon oxides or nitrides, are often necessary in practical devices in order to avoid surface recombination (Sect. 10.12.1) or the interaction with atmospheric oxygen or water.

But surface physics is interesting in its own right, investigating the properties of a complex mostly two-dimensional system. 'Pure' surfaces are studied using crystals cleaved in ultra-high vacuum or carefully prepared atomically clean surfaces. A special case are two-dimensional materials, also termed atomic sheets, such as graphene; these will be discussed in Sect. 13.1.

At the surface the atoms rearrange, compared to their bulk positions, vertically and laterally, also forming new bonds (surface reconstructions). The mechanical properties (surface phonons) and elec-

M. Grundmann, *The Physics of Semiconductors*, Graduate Texts in Physics,
https://doi.org/10.1007/978-3-030-51569-0_11

tronic properties (surface states) are different from the bulk modes. Detailed treatments of surface physics and its experimental methods can be found in [695, 1056–1058].

11.2 Surface Crystallography

The surface symmetry, i.e. the two-dimensional spatial periodicity of the constituent atoms, is described with the ten two-dimensional point groups (Table B.1). The point symmetries are 1-, 2-, 3-, 4-, and 6-fold rotational symmetry (Fig. 3.9) with or without mirror plane(s). The two-dimensional point symmetries of popular substrate orientations are compiled in Table 11.1; the different symmetry of the first layer and the half-space are notable. The combination of five 2D Bravais lattices (cmp. Sect. 3.3.1) with the 10 2D point groups leads to the 17 two-dimensional space groups (wallpaper groups) [1059].

For the treatment of surface in reciprocal space, the three-dimensional $\mathbf{k}$-vector is split into the two-dimensional component $\mathbf{k}_{||}$ parallel and the one-dimensional component $\mathbf{k}_{\perp}$ perpendicular to the surface,

$$\mathbf{k} = \mathbf{k}_{||} + \mathbf{k}_{\perp} \ . \tag{11.1}$$

The three most important Brillouin zones in two-dimensional $\mathbf{k}$-space are depicted in Fig. 11.1. Often the special points of the 2D Brillouin zones are denoted with a bar over the letter.

Table 11.1 Two-dimensional point symmetries of common substrates with ideal low-index surfaces

Crystal	Surface	1st layer	1st & 2nd layers	Half space
Rocksalt	(001)	4 mm	4 mm	4 mm
	(110)	2 mm	2 mm	2 mm
	(111)	6 mm	3 m	3 m
Diamond	(001)	4 mm	2 mm	2 mm
	(110)	2 mm	2 mm	2 mm
	(111)	6 mm	3 m	3 m
Zincblende	(001)	4 mm	2 mm	2 mm
	(110)	1 m	1 m	1 m
	(111)	6 mm	3 m	3 m
Wurtzite	(00.1)	6 mm	3 m	3 m
	(10.1)	2 mm	2 mm	1 m
	(11.0)	2 mm	2 mm	1 m

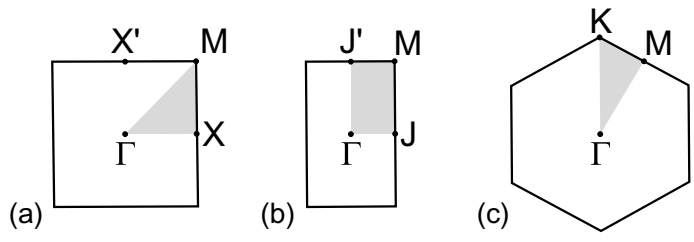

Fig. 11.1 Two-dimensional Brillouin zones for **a** square, **b** rectangular and **c** hexagonal surface symmetry. Special points are labelled and the *grey areas* indicate the smallest irreducible area

11.3 Surface Energy

The surface energy, more precisely the surface energy per area γ, is related to the work that is necessary to split a crystal in two parts. Such process will leave broken ('dangling') bonds. This energy will depend on the crystal orientation as is already clear from the fact that there are easy cleaving planes (Sect. 5.4.2). The surface energy will also depend on the surface reconstruction (see Sect. 11.4), i.e. the rearrangement of surface bonds and atoms. Generally, the reduction of the number of dangling bonds on a surface lowers its energy, while the distortion of bonds increases its energy.

The anisotropy of the surface energy for a given orientation hkl, $\gamma(hkl)$, determines the equilibrium crystal shape (ECS) at a given temperature (below melting temperature). The crystallite is assumed to be of at least mesoscopic size such that energy effects due to edges and apexes can be neglected compared to the surface energy terms. As an example theoretically calculated surface energy values for covalent semiconductors are listed in Table 11.2. The equilibrium shape of silicon has been observed for µm-sized bulbs as shown in Fig. 11.2a for $T = 1323\,K$; the experimental anisotropy of surface energy of silicon is shown in Fig. 11.2b.

11.4 Surface Reconstruction

When in a *Gedankenexperiment* the bulk crystal is split such that a surface with defined orientation develops, many bonds are cut. These dangling bonds can be saturated with other atoms such as hydrogen. In particular under vacuum conditions, the dangling bonds will rearrange and form new

Table 11.2 Surface energy (in J/m^2) for various C, Si and Ge surfaces. Data from [1060]

Material	{111}	{110}	{100}	{311}
C	8.12	7.48	9.72	8.34
Si	1.82	2.04	2.39	2.12
Ge	1.32	1.51	1.71	1.61

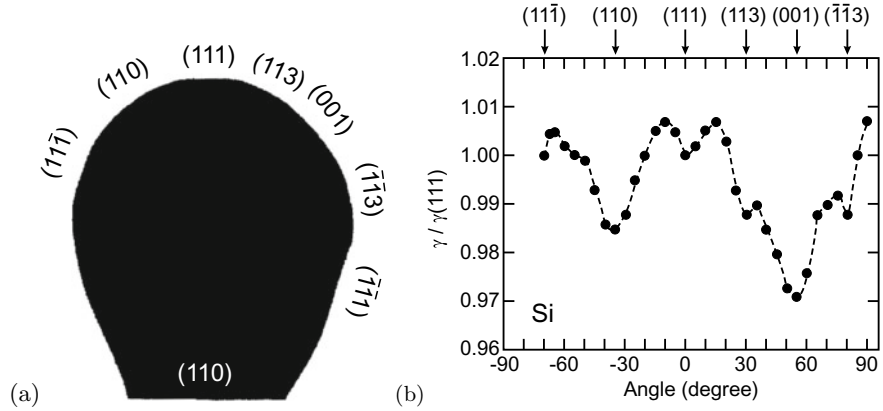

Fig. 11.2 **a** Equilibrium crystal shape (cross section in ⟨110⟩ azimuth) of 1.06 µm diameter Si bulb at $T = 1323\,K$ with facet orientations as labelled. **a** Anisotropy of surface energy (relative to $\gamma(111)$) for Si, the *dashed line* is guide to the eye. Adapted from [1061]

bonds such as dimers along the surface, lowering the total energy. This surface reconstruction displays two-dimensional periodicity of a surface unit cell.

Since the forces from the split-away half-space are missing, the atomic planes will rearrange vertically[1] and the surface-near layers will exhibit slightly different lattice spacing than in bulk. In [1062] the surface reconstructions of many semiconductors are reviewed. In Fig. 11.3a the rearrangement of surface atoms on GaAs(110) is depicted as an example. The anion is moved up, the cation moved down, preserving the bond length, rotating the bond by about $\gamma = 30°$ for various III–V semiconductors [1063] (Fig. 11.3b). The height difference of the top anion and cation Δ_1 scales with the bulk lattice constant (Fig. 11.3c). The details are specific to materials and orientations.

Different reconstructions occur for different thermodynamical conditions, some of them being metastable, as depicted for GaAs(100) in Fig. 11.4. Several different surface reconstructions can also be present simultaneously at a surface within different domains.

The stable reconstruction of the Si(111) surface is the somewhat complicated 7×7 reconstruction which is schematically depicted in Fig. 11.5a as proposed in [1066] ('DAS' dimer-adatom-stacking fault model'). A STM image of this surface has been reported first in [1067] and is depicted in Fig. 11.5b. Details of this surface are also recently a subject of interest [1068].

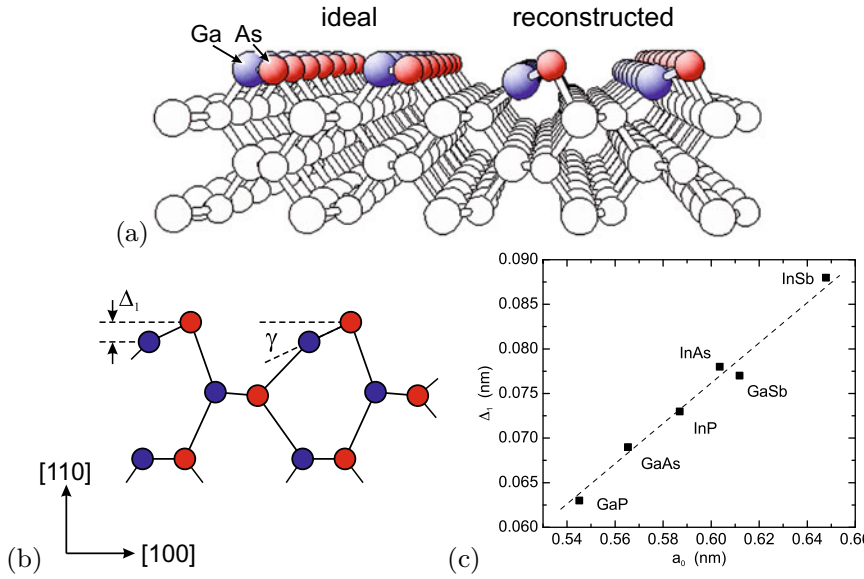

Fig. 11.3 **a** Schematic drawing of the GaAs(110) surface after cutting bonds ('ideal') and actual atomic rearrangement with asymmetric dimer in the reconstructed state. Adapted from [1064]. **b** Schematic of the III–V (110) surface relaxation (*red circles*: anions, *blue circles*: cations) with bond rotation ω and atom shift Δ. **c** Experimental values for he relaxation Δ_1 as shown in panel (**b**) for various semiconductors vs. their bulk lattice constant a_0; *dashed line* is straight line as guide to the eye. Data from [1063]

[1] Typically the distance between the first and second layer is reduced, and the distance between the second and third layer a little bit increased.

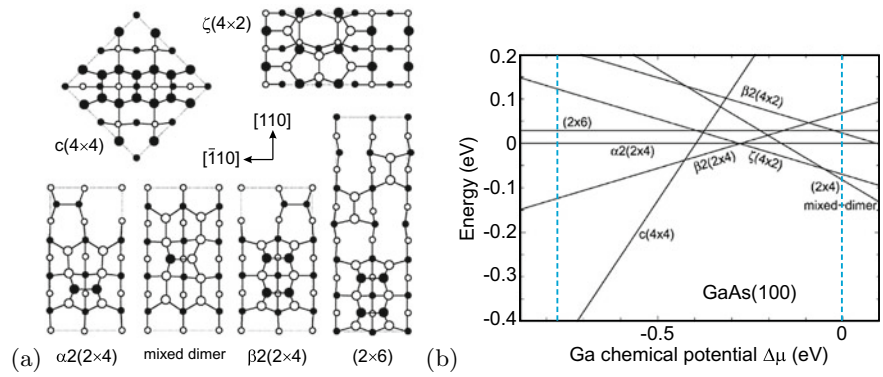

Fig. 11.4 **a** Various reconstructions of the GaAs(100) surface. *Filled* (*empty*) *circles* represent As (Ga) atoms. Atom positions in the top two atomic layers are indicated by *larger symbols*. **b** The relative formation energy per (1×1) unit cell of various reconstructions as a function of the Ga chemical potential. *Vertical dashed lines* mark the approximate anion- and cation-rich limits of the thermodynamically allowed range of $\Delta\mu$. Adapted from [1065]

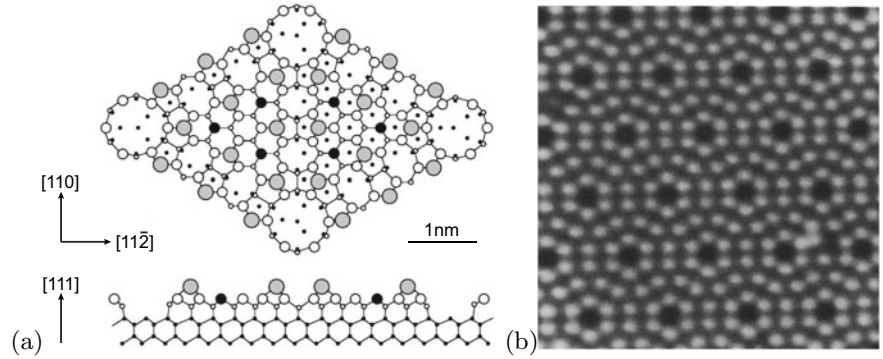

Fig. 11.5 **a** Schematic drawing of the 7×7 reconstruction of Si(111) surface. The *large grey circles* represent adatoms, the *small balck circles* rest atoms. Adapted from [1066] **b** STM image (empty states) of such surface. Adapted from [1067]

11.5 Surface Morphology

The surface reconstruction is related to the local atomic arrangement of the surface atoms. On larger length scales, surfaces can exhibit roughness in general and various specific morphologies, among them steps, step bunches, facets, hillocks or pits. When atomically flat terraces are separated by steps of equal heights, the surface is termed *vicinal*. The step height can be an atomic monolayer or more. The step edges can be straight, smoothly curved or rugged, depending on the formation energy of kinks. If the substrate surface is inclined by a small 'off-cut' angle θ with respect to a low index plane, for a step height h the average terrace width L is given by

$$L = \frac{h}{\tan\theta} \approx \frac{h}{\theta} \,. \tag{11.2}$$

The Si(001) surface (under certain conditions) exhibits monoatomic steps between the A-type 1×2 and B-type 2×1 terraces [1069]; clearly also the step edges between A–B and B–A are quite different, one being much rougher than the other (Fig. 11.6). The surface is thus a two domain surface, the symmetry of both A- and B-type terraces being 2 mm, rotated by 90° against each other.

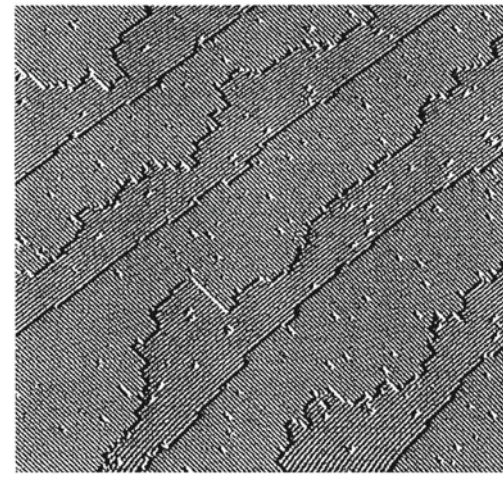

Fig. 11.6 STM image of Si(001) surface with an off-cut $\theta = 0.5°$. Adapted from [1069]

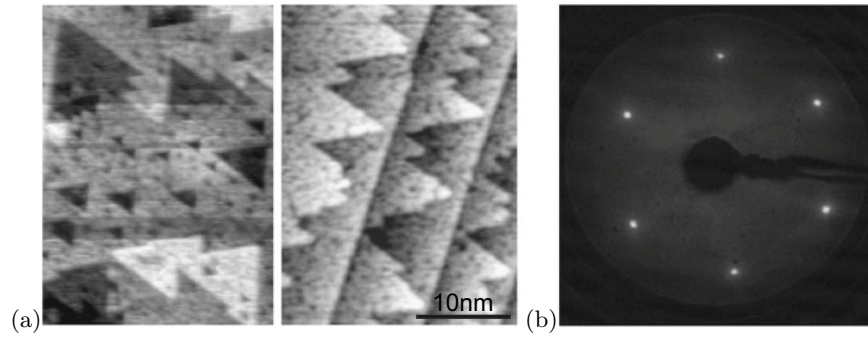

Fig. 11.7 **a** STM images a ZnO(00.1) O-terminated surface, left (right) panel with zero (about 1.3°) off-cut, exhibiting monolayer step heights of 0.27 nm. **a** LEED pattern of such surface (recorded at 70 eV). Adapted from [1070]

A similar example is the Zn(00.1) surface. The found step height of the monoatomic steps is 0.27 nm and corresponds $c/2$ [1070]. The terrace width is about 12 nm (Fig. 11.7a), yielding an off-cut (11.2) of about 1.3°. The surface pattern shows triangular features in two orientations, rotated by 60°. The $3m$ symmetry of the surface, although the first monolayer has 6 m point symmetry (Table 11.1), occurs in two domains rotated against each other by 60°. The LEED pattern from each individual terrace is expected to have three-fold symmetry; the mixed character of the surface yields a six-fold pattern (Fig. 11.7b).

Steps can gather and form step bunches with a height much larger than a monolayer (Fig. 11.8). Faceting of higher index planes occurs when it is energetically favorable to form alternating facets of low energy low index planes, for example Si(223) exhibits periodic ridges with (111) and (113) facets [1071]. The faceting of a surface close to (113), exhibiting smooth (113) and rough (114) planes, is depicted in Fig. 11.9.

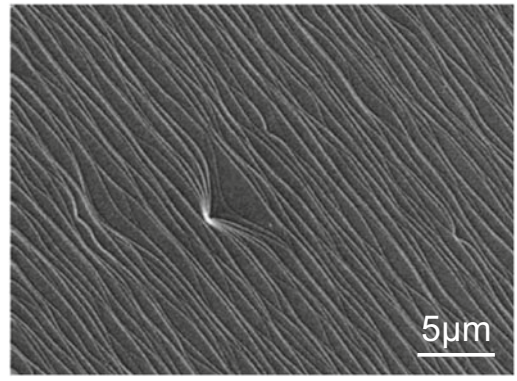

Fig. 11.8 SEM image of the surface of a 4H–SiC layer on [00.1]-oriented substrate with 8° misorientation towards [11.0]. Adapted from [1072]

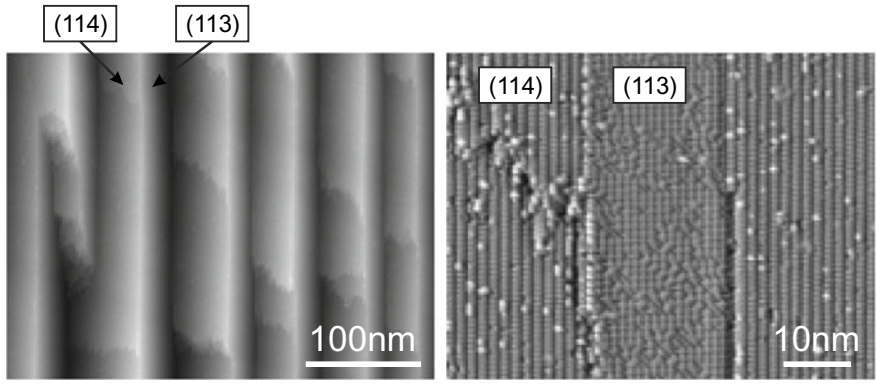

Fig. 11.9 STM images of a silicon surface close to (113), 21.5° from (001) towards (111), i.e. (113)-3.7°. Adapted from [1073]

11.6 Surface Physical Properties

11.6.1 Surface Phonons

As a model for surface vibrational states, the diatomic one-dimensional chain model discussed in Sect. 5.2.2 can be modified to allow for a different surface spring constant C_s instead of C_1 or C_2. Such model can be solved numerically for finite chain length. The bulk dispersion is found with an extra mode in the gap or above the maximum frequency for a range of values of C_s as depicted in Fig. 11.10. When the spring constant of the surface atom is smaller than the larger of the two spring constants C_1 and C_2 (in our model calculation $C_2 > C_1$), a state in the gap forms; for a surface spring constant larger than C_2, first the surface vibration lies within the optical bulk band and then forms a state above the maximum optical frequency ω_m, given by (5.18).[2]

In order to display the dispersion of surface states together with the bulk band structure, the latter is projected to the surface $\mathbf{k}_{||}$-vector: $E_n(\mathbf{k})$ is considered as $E_{n,\mathbf{k}_\perp}(\mathbf{k}_{||}) = E_\nu(\mathbf{k}_{||})$, where $\nu = n$, $\mathbf{k}_\perp$ is a new, continuous index. In the plot of E_n^{surf} vs. $\mathbf{k}_{||}$, for each value of $\mathbf{k}_{||}$ a *range* of energies reflects the

[2]The appearance of states within the gap and above ω_m resembles that of localized vibrational modes of substitutional masses (Sect. 5.2.7).

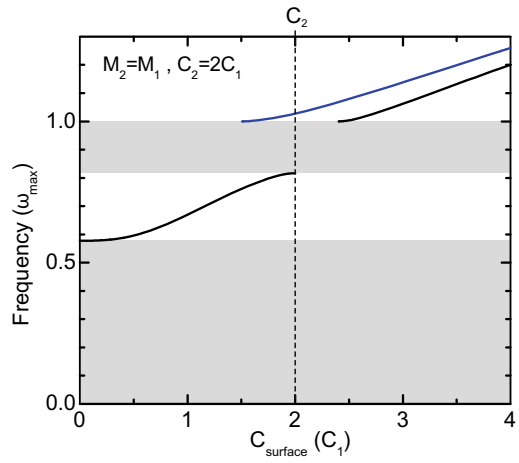

Fig. 11.10 One-dimensional model calculation of surface vibrational state frequency (in units of the maximum bulk optical phonon frequency ω_m) as a function of the spring constant $C_{surface}$ of the surface atom replacing C_1 (*blue curve*) or C_2 (*black curves*). As model parameters we use equal masses and $C_2 = 2\,C_1$ ($\gamma = 0.943$ from (5.17)). The *grey areas* represent the energy range of the acoustic and optical phonon bulk bands

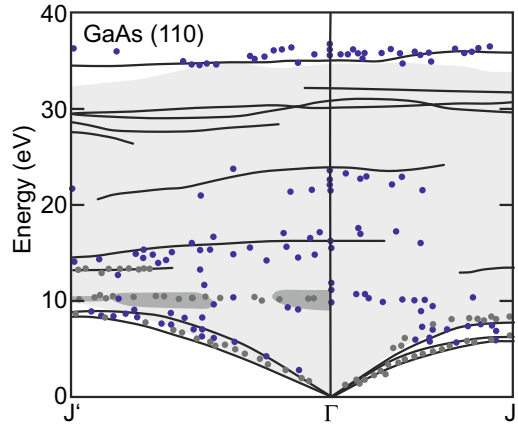

Fig. 11.11 Surface phonon dispersion for GaAs(110) (*solid lines*) with the surface projected bulk band structure (*light grey area*). The *symboles* are experimental data from two different methods. The *dark grey areas* at about 10 meV indicate regions where the A_1-peak is present in the calculated scattering cross-section. Adapted from [1063]

bulk band structure (Fig. 11.11). This concept pertains to phonon dispersion as well as to electronic states.

11.6.2 Surface Plasmons

Free-carrier oscillations in the bulk had been discussed in Sect. 9.9.1. A surface plasmon is the quantum of a surface-bound plasma oscillation. Such effect has been discussed in [1074] and reviewed in [1075, 1076]. A metal (or conductive semiconductor) with dielectric constant according to (9.77) $\epsilon_1 = \epsilon_m = \epsilon_r\,(\omega_p/\omega)^2$ and a dielectric (or vacuum) with $\epsilon_2 = \epsilon_d$ are assumed (Fig. 11.12).

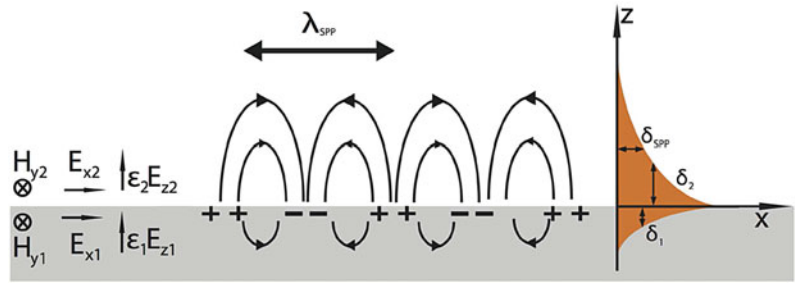

Fig. 11.12 Sketc.h of surface plasmon field distribution. Adapted from [1077]

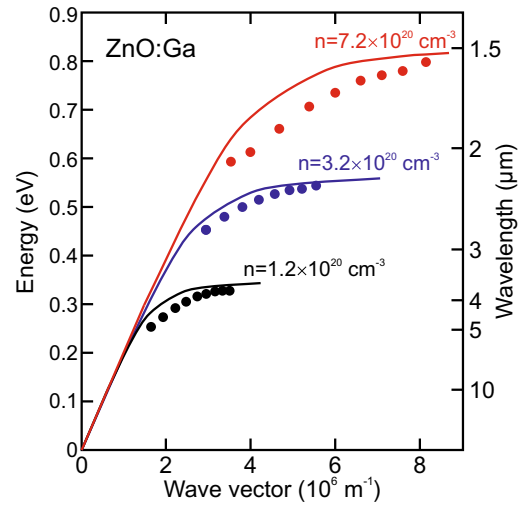

Fig. 11.13 Surface plasmon polariton dispersion for ZnO:Ga/air for three different carrier concentrations as labelled, experimental data (*symbols*) and theory (*lines*). Adapted from [1078]

The surface plasmon (polariton) (SPP) is a wave localized at the surface with evanescent parts into the metal and the dielectric. The dispersion of the surface plasmon (polariton) is given by

$$k_{\mathrm{SPP}} = \frac{\omega}{c}\sqrt{\frac{\epsilon_1\,\epsilon_2}{\epsilon_1+\epsilon_2}}\,. \tag{11.3}$$

For large k, the limiting frequency is the SPP frequency (from $\epsilon_1 = \epsilon_2$)

$$\omega_{\mathrm{SPP}} = \frac{\omega_{\mathrm{p}}}{\sqrt{1+\epsilon_{\mathrm{d}}/\epsilon_{\mathrm{r}}}} < \omega_{\mathrm{p}}\,, \tag{11.4}$$

which is smaller than the plasma frequency. For a metal against vacuum, $\omega_{\mathrm{SPP}} = \omega_{\mathrm{p}}/\sqrt{2}$. The SPP dispersion for a ZnO:Ga/air interface is depicted in Fig. 11.13 for three different doping concentrations.

11.6.3 Electronic Surface States

The bulk band structure is given by the energy eigenvalues $E_n(\mathbf{k})$. The surface adds its own states $E_n^{\mathrm{surf}}(\mathbf{k}_{||})$, many of them in the gap. The calculation of gap states has been already briefly discussed in Sect. 6.2.3. The nature of bulk states is oscillatory in the bulk and exponentially decaying in the outside (Fig. 11.14a), the nature of surface states is localized at the surface and decaying both towards

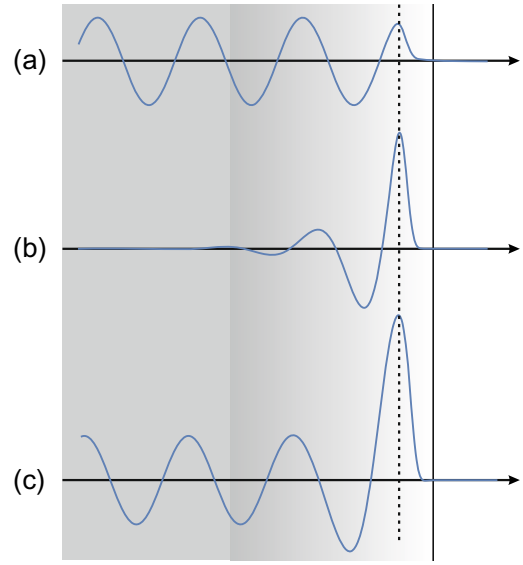

Fig. 11.14 Schematic wavefunction versus coordinate for **a** bulk state in the vicinity of the surface (its position indicated by the *vertical dashed line*), **b** surface state and **c** surface resonance state

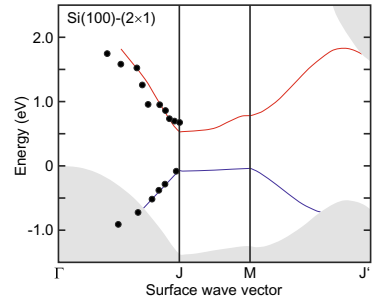

Fig. 11.15 Surface band structure of Si(100)-(2 × 1), *lines* denote a theoretical quasi-particle calculation, *symbols* represent experimental data. The *grey areas* indicate the projected bulk band structure. Adapted from [1079]

the bulk and the outside (Fig. 11.14b). A third type of states is a *surface resonance* which is oscillatory in the bulk and has enhanced probability at the surface, of course also decaying towards the outside (Fig. 11.14c); such states are surface related but energetically degenerate with states of the bulk band structure.

Surface states for Si(100) in 2 × 1 reconstruction are shown in Fig. 11.15. The surface bands arise from (filled and unfilled) π- and π^*-orbitals from the dangling bonds on the threefold-coordinated surface atoms [1079]. A calculation for the ideal (unreconstructed) (100), (110) and (111) surfaces of Si, Ge and GaAs can be found in [1080]. Further work on silicon surface states (clean and with adsorbates) is compiled in [1081].

For a conventional insulating material (with gap) the states of conduction and valence band have defined s- and p-type symmetry (cmp. Fig. 2.5) and the surface states can be populated with spin up and down electrons as is schematically drawn in Fig. 11.16a. Such 'normal' surface states are thus not spin-polarized. This has been shown, e.g., for the well-known surface states of Si(111)-(7 × 7) [1082] in [1083].

In a so-called *topological insulator* [464], a band inversion is present (cf. Sect. 6.2.6). In HgTe-like materials, s- and p-type bands are inverted at the Γ point (cmp. Sect. 6.11). In layered (orthorhombic) Bi_2Se_3-like tri-chalcogenide materials two p_z-orbitals with opposite parity are inverted at the Γ point. Reasons for the band inversion are spin-orbit interaction but also scalar relativistic effects and lattice distortions [1084]. The spin-orbit interaction is responsible for opening a gap; the associated surface

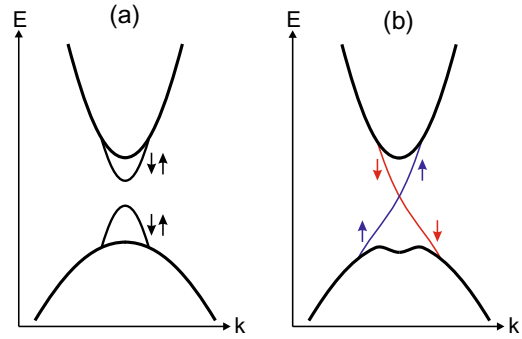

Fig. 11.16 **a** 'Normal' band structure with surface states, the valence band states are antisymmetric ('–') from p-states, the conduction band states are symmetric ('+') from s-states. The *arrows* denote the electron spin orientation of the states. **b** 'Topological' band structure with surface states crossing the gap and electrons in the two surface states having unique spin orientations

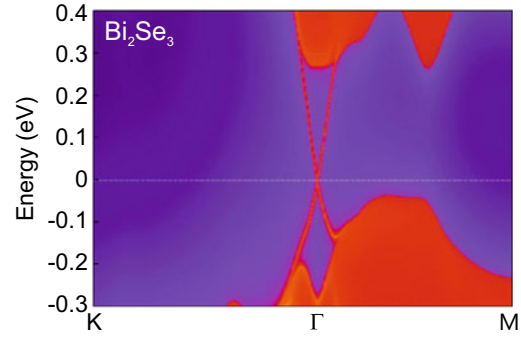

Fig. 11.17 Density of states for Bi_2Se_3 (111) surface. Adapted from [1086]

states cross the band gap (Fig. 11.16b) and are spin-polarized (Fig. 11.16c) [1085, 1086]. A review of various systems is given in [463]. Charge transport in such spin-polarized surface states suffers no scattering (thus these states are called 'topologically protected') unless by a center that breaks time reversal symmetry (magnetic impurity). The more or less linear dispersion of these states forms a 'Dirac cone' (cmp. Sect. 13.1.2 for the band structure of graphene with six Dirac cones) (Fig. 11.17).

Topological surface states have been observed in various systems [463]. As an example we show data on bulk Bi_2Se_3 [1087] for which the surface states are found to cross the band gap (Fig. 11.18a) and spin-polarized measurements (Fig. 11.18b) show a strong spin polarization (about 50%) of the two branches. Another situation where topological edge states appear is the interface between two semiconductors with bands of different topology, such as HgTe and CdTe (cf. Sect. 6.11).

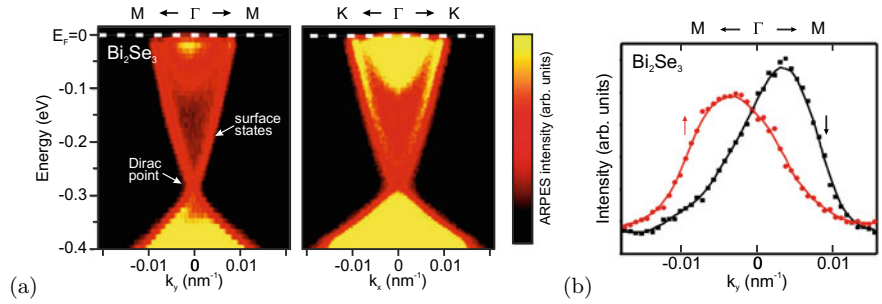

Fig. 11.18 **a** Angle-resolved photoemission spectra from Bi_2Se_3 (111) surface along two different **k**-space directions. The Fermi level is at energy zero. The *blue dashed line* indicates the angular scan displayed in panel (**b**). **b** Spin-polarized momentum distribution curve at a binding energy of −140 meV, measured along the k_y-direction. Adapted from [1088]